Visible Light Communication System for Platooning Applications

Bastien Béchadergue, Hongyu Guan, Luc Chassagne, Samir Tohmé, Jean-Laurent Franchineau

Visible Light Communication System for Platooning Applications

B. Béchadergue[1, 2], H. Guan[1], L. Chassagne[1], S. Tohmé[2], J.L. Franchineau[2]

1: Laboratoire d'Ingénierie des Systèmes de Versailles (LISV), University of Paris Saclay (University of Versailles Saint-Quentin), 10-12 avenue de l'Europe, 78140 Vélizy, France
2: Vedecom Institute, 77 rue des Chantiers, 78000 Versailles, France

Abstract: Vehicle-to-vehicle (V2V) communication is crucial in platooning configurations to ensure lateral and longitudinal control of the vehicle trajectory and thus must be reliable. Though radio frequency (RF) systems are widely used for their numerous qualities, their performances can be severely degraded in dense traffic scenario. Visible light communication (VLC), which is not as sensible, could be used as a complementary technology. In this work, a simple and low-cost VLC system suitable for V2V communications is presented. An off-the-shelf central stop lamp, composed of six low-power light-emitting diodes (LED), is used as emitter whereas a photodiode (PD) coupled with an analog processing circuit is used as receiver. This system provides, at a rate of 100 kbps and without errors, a packet delivery ratio (PDR) of 100% over 4.5 m and 77% over 6 m while keeping the transmission latency under 6 ms and is thus compatible with platooning applications.

Keywords: VLC, V2V, LED, platooning, prototype

1. Introduction

Intelligent transportation systems (ITS) are cornerstones on the road towards vehicle automation and have thus gained strong interest over the last decades. Though they are already enough developed to enable fully autonomous driving, they are appearing only progressively on the market for driving assistance or automation of certain driving phases only. One of this next phase could be platooning.

In platooning, a leading vehicle opens the way to following vehicles that automatically adjust their position using several sensors and data exchange. Since the initial developments in the 1960s [1], there has been extensive research to improve this technique that could increase traffic flow and security [2]. Among other projects, the European initiative Safe Road Train Environment (SARTRE) achieved in 2012 a fully autonomous, infrastructure independent, 5 to 10 m platoon lead by a manually driven vehicle [3]. Vehicle-to-vehicle (V2V) communication is achieved through the radio frequency (RF) technology defined by the IEEE 802.11p standard. IEEE 802.11p can provide long range and high data rate transmission but is also very sensible to interferences and can experience long transmission delays in dense traffic scenario [4]. These delays are critical to set the inter-vehicle distances and if they are too large, these distances have to be increased in order to meet safety requirements. However, SARTRE project found with an aerodynamic study that the optimal inter-vehicle distance is between 6 and 8 meters and the United State Department of Transportation (USDOT) recommends to keep the transmission latency around 20 ms in platooning applications [5].

Visible light communication (VLC) consists in modulating the light produced by light-emitting diodes (LED) to transmit data. On the receiver end, a photodetector, usually a photodiode (PD), converts the light signal into an electrical signal that is then processed to recover the data. Note that the receiver must be in the line-of-sight (LOS) of the receiver to enable communication. VLC has experienced very rapid development since its first steps in the early 2000s and can rely on the progressive replacement of traditional light sources to spread. The transportation field is no exception since LED are now prevailing for both automotive and road infrastructures lighting. VLC has thus naturally been considered as a potential candidate for V2V communication and actually happens to be competitive, especially by satisfying the latency requirements of dense traffic conditions [6] such as platooning [7]. Though several VLC prototypes have already been proposed [8]-[14], only a few dealt with the platoon application. In [15], a 9.5 kbps VLC system is presented and can provide 100% packet-delivery ratio (PDR) over 30 m with a transmission latency of 36 ms by using a custom made LED-based emitter.

In this work, a simple and low-cost VLC system suitable for platooning applications is presented. An off-the-shelf central stop lamp composed of six low-power LED is used as emitter and a PD coupled with an analog processing circuit is used as receiver. This system provides, at a rate of 100 kbps and without errors, a PDR of 100% over 4.5 m and 77% over 6 m while keeping the transmission latency under 6 ms.

The reminder of this paper is organized as follows: Section 2 will give a general presentation of the system and of the free space optical channel whereas Section 3 will enter into the details of the emitter and receiver design. Finally, Section 4 will present the performances of the systems in terms of PDR and latency.

2. The VLC system and its environment

2.1 General working principles of the system

Though the research on VLC prototypes for automotive use is still at an exploratory stage, a general framework has been set through the IEEE 802.15.7 standard [16]. This standard lists several design recommendations for VLC systems, especially concerning the physical (PHY) layer. For outdoor applications, the standards recommends the use of the PHY I layer which supports on-off keying (OOK) modulation and variable pulse-position modulation (VPPM) combined with forward error correction (FEC). Table I sums up the different combinations allowed by the PHI I layer.

Modulation	RLL code	Clock (kHz)	FEC		Data rate (kbps)
			RS	CC	
OOK	Manchester	200	(15,7)	1/4	11.67
			(15,11)	1/3	24.44
			(15,11)	2/3	48.89
			(15,11)	None	73.3
			None	None	100
VPPM	4B6B	400	(15,2)	None	35.56
			(15,4)	None	71.11
			(15,7)	None	124.4
			None	None	266.6

Table I: Detail of the IEEE 802.15.7 PHY I layer [16].

The system proposed in this work transmits, using OOK modulation, Manchester-encoded messages, or packets, at an optical clock rate of 200 kHz, with no FEC. It is thus standard compliant and can achieve a data rate of 100 kbps.

The transmitted messages are built following the recommendations of the USDOT for cooperative forward collision warning systems. Consequently, the length of such messages is set at 400 bits that are randomly generated according to a uniform distribution. Manchester encoding then turns each bit 1 into a symbol of two bits 10 and each bit 0 into the symbol 01, which means there is a maximum run of two zeros between consecutive ones and vice versa. Therefore, the power spectrum of a packet contains several lobes, centered on the odd multiples of the data rate, that is 100 kHz, and with decreasing amplitude as the frequency increases [17]. Finally note that a synchronization frame is added at the beginning of each packet so that the receiver will be able to detect when a new packet is starting.

This packet generation step is the first stage of our VLC system, which general working principles is represented in Figure 1.

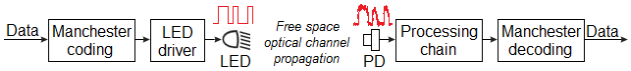

Figure 1: Working principles of the VLC system.

Data generation and encoding is performed by a field-programmable gate array (FPGA), which then turns on and off the transmit LED through an LED driver. This emitter end of the system, which corresponds to the left part of Figure 1, will be further detailed in Section 3.1. After propagation through the free space optical channel, which model will be exposed in Section 2.2, the light signal is received and turned into an electrical signal by a PD. It is then processed by an analog circuit in order to reconstruct the data pulses and sent to another FPGA for decoding. This receiver end of the system, which corresponds to the right part of Figure 1, will be developed in Section 3.2.

The PD and processing chain are critical steps that must be carefully designed to ensure good performances. However, this design depends strongly on the quantity of received light and thus on the LED characteristics as well as the distortions and attenuations introduced by its propagation through free space. These distortions and attenuations can be modelled by the free space optical channel model that is now going to be described.

2.2 The free space optical channel model

The free space optical channel model gives a theoretical representation of a typical VLC link where the receiver is in the LOS of the emitter and the atmosphere is clear. It corresponds to a classical path-loss Additive White Gaussian Noise (AWGN) channel model [1], where the photocurrent produced by the PD is related with the average optical power transmitted by the LED $X(t)$ through the formula:

$$Y(t) = \gamma X(t) \otimes h(t) + n(t), \qquad (1)$$

where γ is the PD responsivity, $h(t)$ is the channel impulse response and $n(t)$ is the AWGN. The channel frequency response $H(f)$, considered flat in the frequency range of interest, can be limited to its DC gain $H(0)$, defined for Lambertian light source as:

$$H(0) = \frac{(m+1)A_r}{2\pi D^2}\cos^m\varphi\cos\psi, \quad \text{when } 0 < \psi < \psi_c, \qquad (2)$$

where D, φ and ψ are respectively the inter-vehicle distance, the irradiance angle and the incidence angle, A_r is the radiant sensitive area of the PD, ψ_c is the PD field of view and m is the order of Lambertian emission, defined as $m = -\ln 2 / \ln(\cos\phi_{1/2})$, where $\phi_{1/2}$ is the semi-angle at half illuminance of the LED emitter. If the transmitted optical power is P_t, then the received light power P_r will be:

$$P_r = H(0)P_t, \qquad (3)$$

and the received signal power S will be $S = \gamma^2 P_r^2$.

The previous equations describe the path-loss face of the model. The AWGN on the other hand comes from the noises appearing in the PD that are mainly shot noise and thermal noise. Shot noise is induced by the incident luminous flux produced by the light source of interest and background light sources such as daylight, infrastructures light sources or vehicle lamps. Background light sources are usually dominant so shot noise is considered signal independent and thus modelled as a white Gaussian noise with variance σ_{shot}^2:

$$\sigma_{shot}^2 = 2q\gamma P_r B + 2q\gamma I_{bg} I_2 B, \qquad (4)$$

where q is the electronic charge, B is the equivalent noise bandwidth, I_{bg} is the background photocurrent and I_2 is a noise bandwidth factor. The first term is thus the contribution of the light source of interest whereas the second term is the background noise. Thermal noise is also signal independent because induced by charge carriers thermal agitation and is modelled as white Gaussian noise with variance σ_{th}^2:

$$\sigma_{th}^2 = \frac{8\pi k T_K}{G}\eta A_r I_2 B^2 + \frac{16\pi^2 k T_K \Gamma}{g_m}\eta^2 A_r^2 I_3 B^3, \qquad (5)$$

where k is Boltzmann's constant, T_K is absolute temperature, G is the open-loop voltage gain, η is the fixed capacitance of photo detector per unit area, Γ is the FET channel noise factor, g_m is the FET transconductance and I_3 is a noise-bandwidth factor. The total noise variance N will then simply be the sum of shot noise and thermal noise $N = \sigma_{shot}^2 + \sigma_{thermal}^2$. Consequently, the signal-to-noise ratio (SNR) will be:

$$SNR = \frac{S}{N} = \frac{\gamma^2 H(0)^2 P_t^2}{\sigma_{shot}^2 + \sigma_{thermal}^2}. \qquad (6)$$

3. System implementation

3.1 VLC emitter

The VLC emitter, quickly described in Section 2.1, is now going to be fully detailed. In order to keep the system as close as possible to reality, the emitter is implemented using an off-the-shelf central stop light bought to an automotive equipment supplier. As shown in Figure 2, this light is composed of six red LED and its characteristics – the optical power and transmission pattern in particular – are completely unknown. Since the VLC link performances vary widely with these parameters, the first step is to fully characterize the stop light in real working conditions.

Here, the stop light is driven by a Terasic DE0-Nano FPGA board and a direct current (DC) power supply through a specific electronic circuit. The FPGA board produces the data signal, where the logic levels 1 and 0 are respectively represented by high and low voltage levels. This electrical signal controls the gate of a MOSFET transistor that acts as a simple switch letting the current of the power supply flow through the stop light or not.

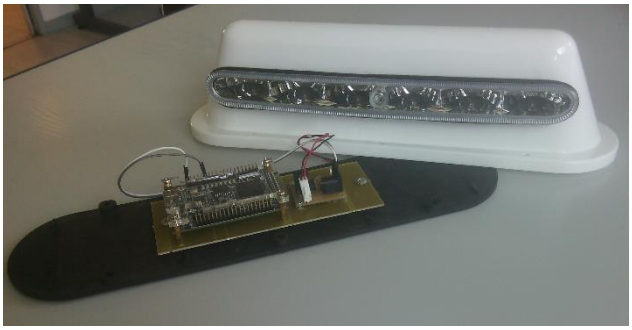

Figure 2: The VLC emitter composed of the central stop light and its driver connected to the FPGA.

As said earlier, the expected clock rate is 200 kHz so the whole emitter must be able to turn on and off at this speed without any problem. LED are known to have bandwidths of at least several megahertz. Consequently, the limiting component in the emitter is here the driver. Using a 50 MHz bandwidth Thorlabs PDA8A photoreceiver, the emitter bandwidth can be tested. Figure 3 shows the signal observed with this photoreceiver when the emitter is driven by a square signal of frequency 200 kHz. The driver clearly fulfils its role since the square signal to transmit is accurately reproduced, especially in terms of rising and falling times and duty cycle.

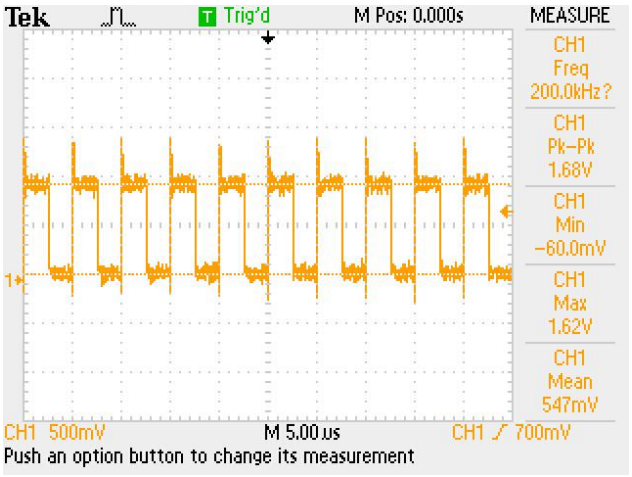

Figure 3: Signal observed with the PDA8A when the VLC emitter transmits a square signal of frequency 200 kHz.

Using this emitter topology, the stop light can now be tested in order to retrieve its photometric characteristics. The test consists here in driving the light at 200 kHz and measuring its illuminance in the same horizontal plane at different points of a 10x4 meters dark room using a TES 1335 luxmeter. Note that since the LED are driven using a square signal with 50% duty cycle, the mean output optical power is only half the maximum output optical power. In order

to evaluate the optical power received by the PD at these different points, the corresponding illuminances were first converted into luminous flux by simply multiplying them by the PD active area A_r. Then, these values were converted into optical power using the method described in [19]. The resulting optical power distribution is presented in Figure 4(a). It appears clearly that except in the near vicinity of the emitter, the received optical power is between 10 and 100 nW. Figure 4(b) gives the detail of Figure 4(a) in the normal axis of the emitter, that is when $\varphi = \psi = 0$. Though the transmission performances also depend on the receiver design, the received optical power seems too weak to expect a reliable VLC link over 10 meters. Note that the illuminances data can be used to deduce the semi-angle at half-illuminance $\phi_{1/2}$, which is in this case 20° and thus corresponds to a Lambertian emission order $m \approx 11$. Then, by fitting the theoretical path-loss model (3) with the experimental data, the transmitted optical power can be estimated at 60 mW, as shown by the red curve on Figure 4(b).

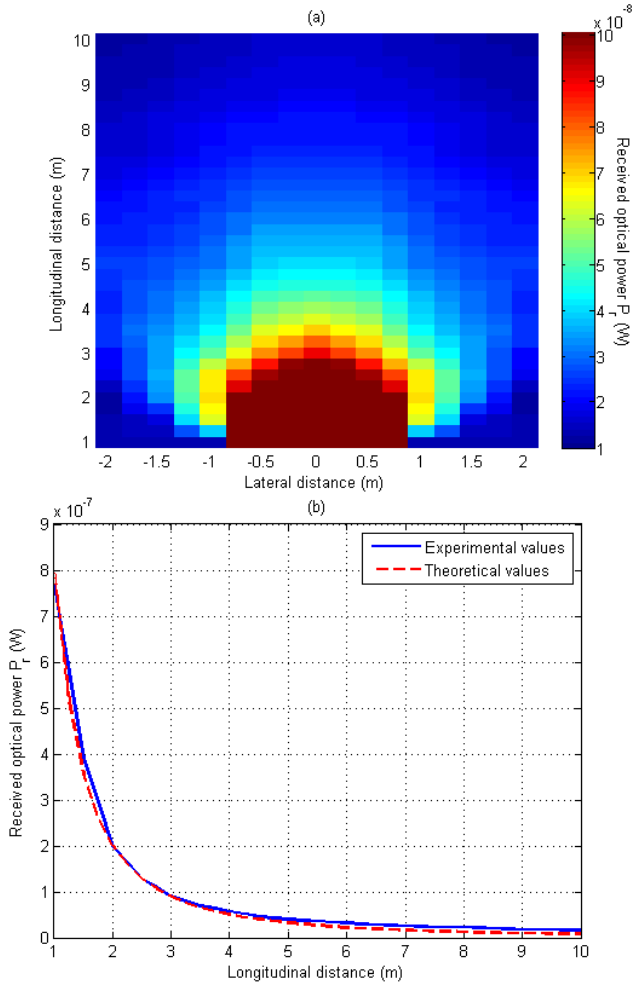

Figure 4: (a) Received optical power distribution on the LED stop light horizontal plane, (b) detail of (a) in the light normal axis (blue) and corresponding theoretical values with $P_t = 60$ mW (red).

3.2 VLC receiver

On the other side of the VLC link, the receiver must be able to detect the transmitted optical signal and reconstruct it. This processing chain is achieved here using the system presented in Figure 5 [12] and implemented using analog components only. A PD converts the optical power it receives into a current that is then transformed into a voltage with a transimpedance amplifier (TIA). The resulting signal is bandpass filtered, amplified and finally triggered using a comparator in order to reconstruct a square signal that is then sent to a DE2-115 FPGA Board for decoding.

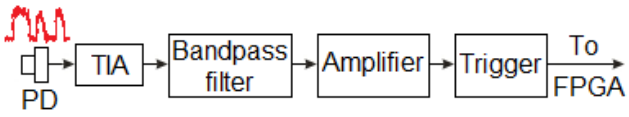

Figure 5: Block schematic of the VLC receiver.

The processing chain must basically remove as much noise as possible while amplifying the signal of interest so that the comparator can work properly. Consequently, the front-end stage, composed of the PD and TIA, is the first critical stage since it must provide as much gain as possible while maintaining a sufficient bandwidth to preserve the power of the received signal. Here, the gain is set at 50 dB while the bandwidth is 400 kHz. Note that the front-end stage will thus behave like a lowpass filter and thus remove a small part of the transmitted message power. Then, the filtering stage is the second critical stage especially in the cut-off frequencies choice. Increasing the passband will preserve a larger part of the signal power but also of the noise. This trade-off is here solved using a first order bandpass filter of 90 kHz passband with an upper cut-off frequency of 100 kHz. Note that the use of active filtering also provides additional gain. Finally, the amplifier stage adds 10 dB of gain just before the hysteresis comparator reconstructs the square pulses and adapt them so that they can be sent to the FPGA.

This processing chain is illustrated by Figure 6 which corresponds to the loop transmission of the data bits sequence 100110 at 10 m in an indoor environment. Figure 6(a) represents the signal given by the front-end stage. This time domain signal is too weak to be clearly identified but the filtering stage, whose output is given in Figure 6(b), allows to detect every pulse. Note that the pulses corresponding to two successive ones or zeros are larger and stronger than the ones corresponding to just one bit. The edges are not as sharp as at emission which is due to the 100 kHz upper cut-off frequency that only preserve the fundamental frequency of the data signal. Figure 6(c) shows that after the amplification stage, the signal is well conditioned for triggering. Finally, this last step is able to reconstruct the square data signal properly, as shown in Figure 6(d).

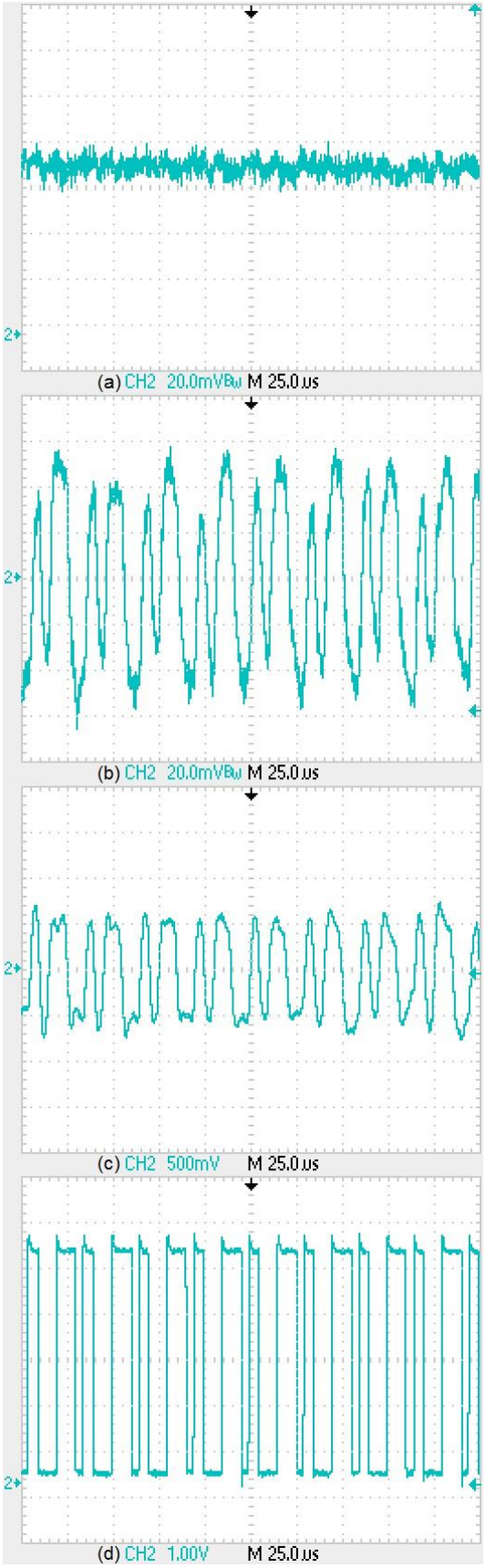

Figure 6: Time evolution of a data signal after (a) the front-end stage, (b) the filtering stage, (c) the amplification stage and (d) the triggering stage.

However, note that the pulses corresponding to a single or two successive ones and zeros have a slightly variable width. This pulse width distortion can have a non-negligible impact and must be taken into account during the decoding process. Here, the decoding is achieved using pulse width measurement [12]. A 50 MHz clock coupled with a counter is used to measure the width of each high level or low level pulse. Figure 7 shows the resulting distribution of the count values when this method is used. There are two main groups on the left and small groups on the right. The first group on the left corresponds to the width of a single bit whereas the second group on the left corresponds to the width of two consecutive bits. Then, the count values on the right correspond to the synchronization frames. Since all the groups are distinct, a simple thresholding can be used to recover the data signal.

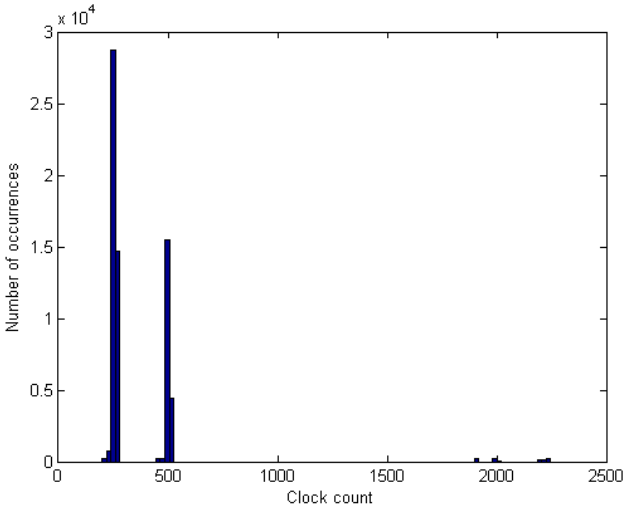

Figure 7: Histogram of the data pulse widths.

4. System performances

Now that our VLC system has been fully described, its performances can be evaluated. The experimental setup used for these evaluations is presented in Section 4.1 whereas the quality of transmission is tested in Section 4.2. Finally the transmission latency is measured is Section 4.3.

4.1 Experimental setup

In order to evaluate the different performances of our system, several experiments were carried out. Using a custom made test bench, the emitter was placed 1.3 m above ground on a first fixed module, as shown by Figure 8. The receiver on the other hand was placed on the same horizontal plane on the second mobile module represented in Figure 9. All the tests were carried out in an indoor environment because the sunlight was too high to obtain exploitable results over 3 m. This is partly due to the fact that the central stop light is too weak in terms of optical power to be used

alone outside and also that no optical filtering and focusing device was used in front of the receiving PD to mitigate the effect of sunlight. Finally note that the message sent during the different tests were as described in Section 2.1.

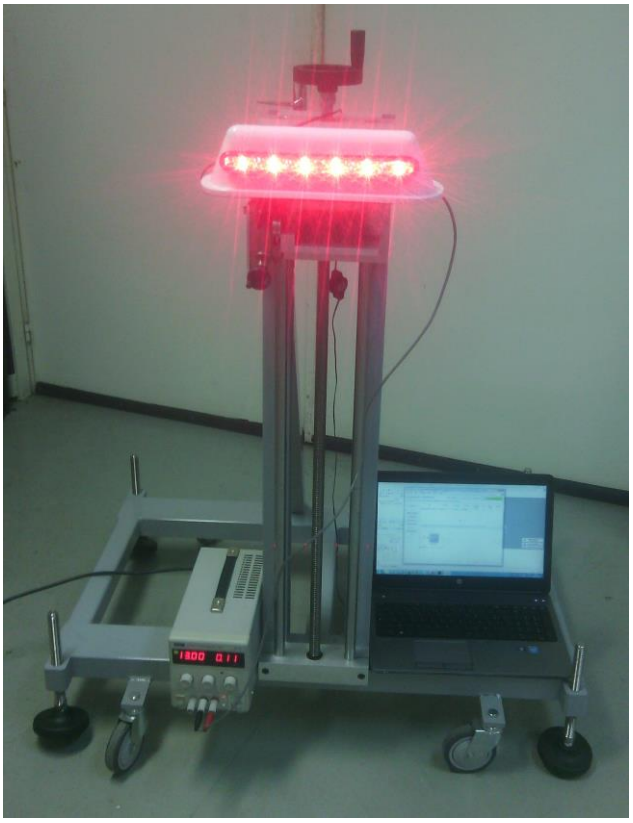

Figure 8: Emitter module used for the experiments: the central stop lamp is at 1.3m above ground and driven by a 13V/110mA DC source.

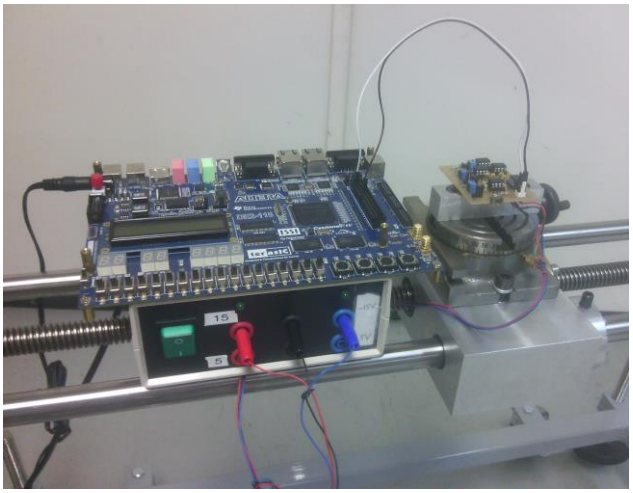

Figure 9: Receiver module used for the experiments. The processing circuit is on the right, connected to the DE2-115 FPGA and powered by a symmetrical +/-15V power supply.

4.2 Transmission quality

In order to be used in a platooning configuration, the present system must be able to transmit as much messages as possible without errors. This ability was here measured by transmitting 425 packets of 400 bits and measuring two different parameters: the percentage of received packets, or PDR, that is the packets which synchronization frame was properly detected, and the percentage of received packets without errors, called here error-free PDR. Figure 10 shows the evolution of these two parameters as the distance between transmitter and receiver increases.

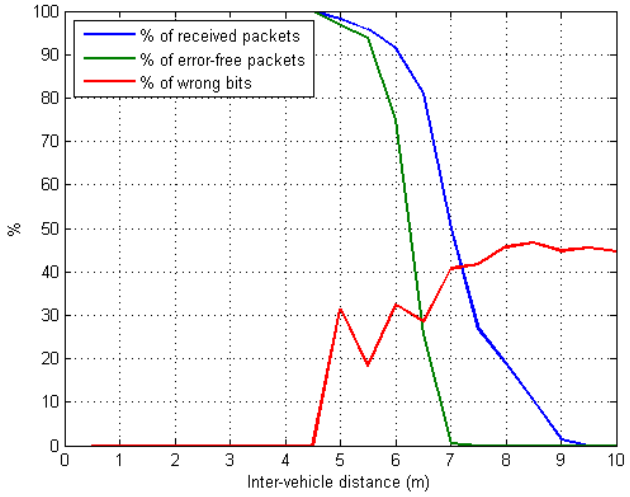

Figure 10: Tests results of the evolution with the distance of the PDR (in blue), the error-free PDR (in green) and the percentage of wrong bits in a packet received with errors (in red).

It can be seen that the system is perfectly functional up to 4.5 m and remains reliable up to 6 m, where the PDR is 90% and the error-free PDR is still 77%. From this distance however, the performances drop dramatically and the system is down from 7 m.

Note also that the share of wrong bits per received packets with error is not varying much but is always high. This is due the pulse width measurement decoding method. If the pulse distortion is too critical, the width of a signal bit 1, for example, could fall on the bad side of the threshold and thus be decoded as two consecutive 1, which will shift the following bits and thus result in a cascade of errors only stopped by the synchronization frames. Consequently, a single error can lead to a large number of errors, which is confirmed by the red curve of Figure 10.

Finally, the error-free transmission range of 6 m may seem rather short. However, note that this value is obtained by only using the central stop light that is, as seen in Section 3.1, quite limited in terms of optical power. This achievable range could be improved by simply using the two taillights in addition to the central stop light.

4.3 Transmission latency

The final tests to conduct are related to the message transmission latency. The latency is defined as the time between the transmission of the first bit of a packet and the moment this packet has been fully received. In order to evaluate the latency, the FPGA on the emitter side was programmed to send a single message when a button is pressed whereas the FPGA on the receiver side was programmed to set an enable bit at a high level when the message is fully received and Manchester-decoded. Figure 11 shows an example of such a message transmission. The orange trace shows the full packet with a synchronization frame at the beginning of the message and an additional synchronization frame at the end so that the message is clearly visible. The blue trace corresponds to the enable bit state. The latency is thus the time delay between the first rising edge in the message signal and the rising edge of the enable bit.

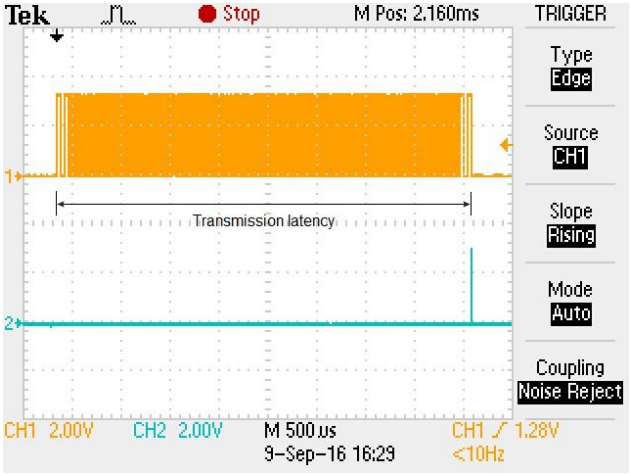

Figure 11: Example of transmission latency, measured as the time between the first rising edge of the message (in orange) and the rising edge of the enable bit (in blue).

In our case, the latency is measured at 4.2 ms which actually corresponds to the number of bits transmitted times the clock rate. In other word, the measured latency corresponds only to the time needed to transmit all the bits of the message and thus depends on the packet length. Note that the definition of latency used here implies that the whole packet should be received and decoded before the information is known. However, the system decodes the data as soon as they are received. If different information are transmitted in the same packet, some information will thus be known before others. In this sense, the latency is further reduced. There is however an incompressible time corresponding to the synchronization frame. This frame is actually a very light transmission protocol that can be used because VLC does not need – yet – heavy protocols like in IEEE 802.11p.

The propagation and reception delays are other incompressible latencies but they do not appear in the measured values because they fall under the time measurement resolution of the oscilloscope. The propagation delay is anyway so low – for example 33 ns at 10 meters – that it can be neglected. The reception delay on the other hand was measured by refining the time resolution of the oscilloscope and is around 3.6 µs. This delay is mainly introduced by the processing chain and especially the bandpass filter.

Note that the latency of 4.2 ms is only effective in perfect conditions, that is when every packet is received without error. As seen in Section 4.2 however, the error-free PDR decreases with the distance. Consequently, considering the same message is sent repeatedly, the latency of good reception can be corrected by taking into account this percentage. This corrected latency is presented in Figure 12. It shows that our system is well suited for platooning applications since the latency, after correction, remains under 6 ms up to 6 meters and thus stays far under the recommended 20 ms.

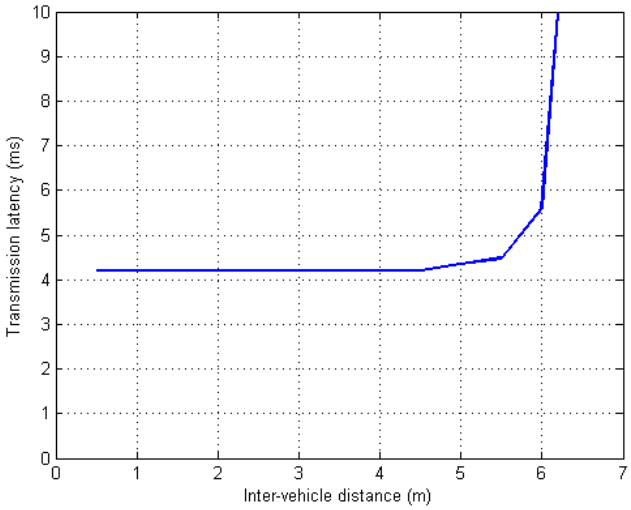

Figure 12: Evolution with the distance of the corrected transmission latency.

5. Conclusion and future works

This paper presents a VLC prototype that aims to be used in platooning applications. Such applications requires a covering range of around 6 meters and a transmission latency of 20 ms. Our system, which working principles and design have been fully detailed here, was tested indoor in order to determine its performances. It is able to receive without error 100% of the transmitted packets up to 4.5 m and 77% up to 6 meters, despite the low optical power of the transmitter. The ideal latency is 4.2 ms, corrected at around 6 ms at 6 m, which is far under the required 20 ms for platooning applications.

However, in order to be fully functional in real tests, the range of our system must be improved such as its robustness to sunlight. Consequently, future work will consist in using the taillights in addition to the central stop light to increase the transmitted optical power. On the receiver side, the careful design of an optical front-stage performing optical filtering and increasing the light collection by the PD will be carried out.

6. References

[1] S. Tsugawa, “An overview on control algorithms for automated highway systems,” in Proc. IEEE/IEEJ/JSAI ITSC, 1999, pp. 234-239.

[2] C. Bergenhem, S. Shladover, E. Coelingh, C. Englund, and S. Tsugawa,“Overview of platooning systems,” in Proc. 19th ITS World Congress,2012.

[3] P. S. Jootel. (2013, Jan.). SAfe Road TRains for the Environment - Final Report. SARTRE Project. U.K. [Online] Available: http://www.sartre-project.eu/en/publications/Sidor/default.aspx.

[4] A. Böhm, M. Jonsson, and E. Uhlemann, “Performance comparison of a platooning application using the IEEE 802.11p MAC on the control channel and a centralized MAC on a service channel,” in Proc. 9th IEEE WiMob, 2013, pp. 545-552.

[5] United State Department of Transportation (2005, March). Vehicle Safety Communications Project Task 3 – Final Report. U.S. [Online] Available: http://ntl.bts.gov/lib/jpodocs/repts_te/14136.htm

[6] C. B. Liu, B. Sadeghi, and E. W. Knightly, “Enabling Vehicular Visible Light Communication (V2LC) Networks,” in Proc. 8th ACM VANET, 2011, pp. 41-50.

[7] M. Y. Abualhoul, M. Marouf, O. Shagdar, and F. Nashashibi, “Platooning control using visible light communications: A feasibility study,” in Proc. 16th IEEE ITSC, 2013, pp. 1535-1540.

[8] M. Akanegawa, Y. Tanaka, and M. Nakagawa, “Basic study on traffic information system using LED traffic lights,” IEEE Trans. Intell. Transp. Syst., vol. 2, no. 4, pp. 197-203, Dec. 2001.

[9] S. Iwasaki, C. Premachandra, T. Endo, T. Fujii, M. Tanimoto, and Y. Kimura, “Visible light road-to-vehicle communication using high-speed camera,” in Proc. IEEE IV’08, 2008, pp. 13-18.

[10] I. Takai, T. Harada, M. Andoh, K. Yasutomi, K. Kagawa, and S. Kawahito, “Optical Vehicle-to-Vehicle Communication System Using LED Transmitter and Camera Receiver,” IEEE Photonics J., vol. 6, no. 5, pp. 1-14, Oct. 2014.

[11] N. Kumar, N. Lourenco, D. Terra, L. N. Alves, and R. L. Aguiar, “Visible light communications in intelligent transportation systems,” in Proc. IEEE IV’12, 2012, pp. 748-753.

[12] A.-M. Cailean, B. Cagneau, L. Chassagne, M. Dimian, and V. Popa, “Novel Receiver Sensor for Visible Light Communications in Automotive Applications,” IEEE Sens. J., vol. 15, no. 8, pp. 4632-4639, Aug. 2015.

[13 K. Cui, G. Chen, Z. Xu, and R. D. Roberts, “Line-of-sight visible light communication system design and demonstration,” in Proc. 7th IEEE/IET CSNDSP, 2010, pp. 621-625.

[14] S.-H. Yu, O. Shih, H.-M. Tsai, N. Wisitpongphan, and R. Roberts, “Smart automotive lighting for vehicle safety,” IEEE Commun. Mag., vol. 51, no. 12, pp. 50-59, Dec. 2013.

[15] M. Abualhoul, O. Shagdar and F. Nashashibi, “Visible Light Inter-Vehicle Communication for Platooning of Autonomous Vehicles,” in Proc. IEEE IV’16, 2016.

[16] S. Rajagopal, R. D. Roberts, and S.-K. Lim, “IEEE 802.15.7 visible light communication: modulation schemes and dimming support,” IEEE Commun. Mag., vol. 50, no. 3, pp. 72-82, Mar. 2012.

[17] I. Glover and P. M. Grant, Digital Communications, 3rd ed. Pearson Education, 2010.

[18] J. M. Kahn and J. R. Barry, “Wireless infrared communications,” Proc. IEEE, vol. 85, no. 2, pp. 265-298, Feb. 1997.

[19] B. Hussain, X. Li, F. Che, C. P. Yue, and L. Wu, “Visible Light Communication System Design and Link Budget Analysis,” *J. Light. Technol.*, vol. 33, no. 24, pp. 5201–5209, décembre 2015.

7. Glossary

AWGN: Additive white Gaussian noise
CC: Convolutional code
DC: Direct current
FEC: Forward error correction
FPGA: Field programmable gate array
IEEE: Institute of Electrical and Electronics Engineering
ITS: Intelligent transportation systems
Kbps: Kilobits per seconds
LED: Light-emitting diode
LOS: Line-of-sight
MOSFET: Metal Oxide Semiconductor Field Effect Transistor
OOK: On-off keying
PD: Photodiode
PDR: Packet delivery ratio
PHY: Physical (layer)
RF: Radio frequency
RLL: Run-length limited
RS: Reed-Solomon
SARTRE: Safe Road Train Environment
TIA: Transimpedance amplifier
USDOT: United State Department of Transportation
V2V: Vehicle-to-vehicle
VLC: Visible light communication
VPPM: Variable pulse-position modulation